Nonreciprocity detector arrays for high-efficiency detection of itinerant microwave photons

Suirong He, Penghui Ouyang, Haiyan Gao, Yufen Li, Jiaxing He, and L. F. Wei*

Information Quantum Technology Laboratory, International Cooperation Research Center of China Communication and Sensor Networks for Modern Transportation, School of Information Science and Technology, Southwest Jiaotong University, Chengdu 610031, China

(Received 4 December 2023; accepted 29 May 2024; published 24 June 2024)

Microwave single-photon detection is one of the critical tasks for the implementation of the desired microwave quantum information processing. Given the detection efficiency of the demonstrated microwave single-photon detector is still very limited, here, we propose a nonreciprocity detector array to implement high-efficiency detection of a single itinerant microwave photon, transported along a one-dimensional waveguide. We show that different from the reciprocity array with more than 20 atomic detectors [Romero *et al.*, Phys. Rev. Lett. **102**, 173602 (2009)] for ideal detection, the nonreciprocity array with just three atomic detectors is sufficient to achieve deterministic detection (i.e., the achievable probability approaches 100%) of a single itinerant microwave photon. Specifically, we design an array with a few current-biased Josephson junctions individually coupled to a common microwave transmission line and then discuss its feasibility.

DOI: 10.1103/PhysRevA.109.062430

I. INTRODUCTION

It is well known that single-photon detection plays a central role in optical quantum computing, quantum sensing, quantum communication [1–4], etc. In fact, a series of single-photon detectors, such as avalanche diodes [5], superconducting nanowires [6], kinetic inductance detectors [7], and superconducting transition edge sensors [8], has been well developed, with excellent performance, for various quantum information processes in the optical-frequency band. However, although the energy of a single microwave photon is significantly low, i.e., 4–5 orders of magnitude lower than that of an optical photon, the detection of a single microwave photon is still a great challenge [9]. Traditionally, weak microwave signals have been received by using a photoconductive antenna and thermoelectric detectors. However, to detect single microwave photons at a single-quantum level, single-detector atoms, whose excited eigenfrequencies are in the microwave frequency band, basically must be engineered for resonant absorption implementations of single microwave photons [9].

Benefitting from experimentally demonstrated artificial atoms (such as superconducting Josephson-junction circuits, semiconducting quantum dots, NV centers, and Rydberg atoms), in recent years, the detection of a single microwave photon has become a feasible and hot topic, specifically because of its central applications in microwave quantum information processing fields [10–12]. Indeed, a series of experiments using the strong interaction between standing-wave photons and artificial atoms [13] demonstrated the high-efficiency detection of standing-wave photons stored in high-quality microwave cavities or resonators. Nevertheless, these approaches cannot be applied directly to detect the itinerant microwave photons due to their delocalizations. In fact, it has been shown [14] that, due to the very weak interaction and impedance mismatch between the traveling-wave microwave photons and the atomic detector, the theoretical upper limit of the detection efficiency is just 50% for a single itinerant microwave photon being detected by a bare atomic detector.

Physically, certain composite systems can be utilized to beat such a 50% detection efficiency limit. For example, cavity- and resonator-atom systems can be constructed to improve the detection probability by overcoming the impedance-mismatch problem between the traveling-wave microwave photon and the atomic detectors [15–25]. More simply, a series of atomic detectors can be arranged as a periodic array to enhance the chance of the photon being detected by one of the detectors [14,26–29]. As shown in [14,26], a single itinerant microwave photon (transported along a one-dimensional waveguide) can be detected with the probability tending to 100% if more than 20 atomic detectors are arranged periodically as an array. Certainly, this is not economical for practical application.

In the present work, we propose a more effective method to utilize the ideal detection of a single itinerant microwave photon by alternatively using a nonreciprocal atomic-detector array that contains just a few atomic detectors. Here, the nonreciprocity means that the electromagnetic waves propagating along opposite directions reveal different losses and phase shifts [30–32]. In fact, such a novel feature was utilized to generate a series of novel electromagnetic devices, including novel optical isolators, circulators, and directional amplifiers [33]. Different from the usual method to realize the electromagnetic nonreciprocity by using the magnetic field,

*Contact author: lfwei@swjtu.edu.cn

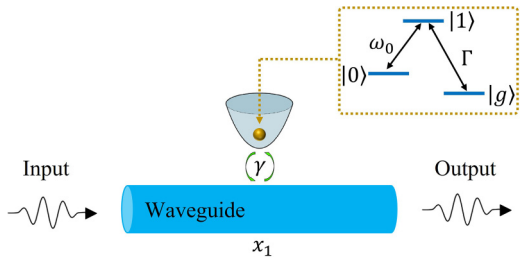

FIG. 1. Schematic diagram of the waveguide photons being scattered by three-level atoms (single-photon detector) located at x_1. Here, V represents the coupling strength between the atom and waveguide photon. ω_0 is the transition frequency between ground state $|0\rangle$ and excited state $|1\rangle$, and Γ is the dissipation rate from the excited state $|1\rangle$ to the final steady state $|g\rangle$.

spatiotemporal modulations, and nonlinearity [30], here, the electromagnetic nonreciprocity is simply realized by using the asymmetric couplings between the atomic detectors and the traveling-wave photons, the different dissipation rates of the atomic detectors, and also the aperiodic arrangement of the detectors. Benefitting from such nonreciprocity, the transmitted and reflected probabilities of the itinerant photons incident from the different directions can be engineered well to realize the ideal impedance match. As a consequence, the itinerant microwave photons can be deterministically detected, at least theoretically.

This paper is organized as follows. In Sec. II, we briefly review why the detection efficiency cannot surpass 50% for a single traveling-wave microwave being detected by either a single three-level atomic detector or a detector generated by two interacting three-level atoms. Focusing on the difficulty the reciprocity array has with economically improving the detection of a single microwave photon, in Sec. III we demonstrate how a nonreciprocity array containing just three atomic detectors can achieve the deterministic detection of a single itinerant microwave photon. Possible physical implementations of the proposal are demonstrated in Sec. IV. Finally, in Sec. V we summarize our work.

II. DETECTION EFFICIENCY LIMIT OF A SINGLE MICROWAVE PHOTON BEING DETECTED BY A SINGLE ATOMIC-TYPE DETECTOR

In this section, we first review the basic model of single itinerant photons and demonstrate that its detection efficiency cannot surpass 50% theoretically with a single atomic-type detector, generated by either a single three-level atom or two interacting ones.

A. Single-photon detection with a single three-level atomic detector

The simplest traveling-wave photon detector can be described by the configuration shown in Fig. 1, where a three-level atom can be resonantly excited by the incident traveling-wave photon (which is expected to be detected) from the initial state $|0\rangle$ into state $|1\rangle$. The photon detection is then implemented by probing the population of the atomic state $|1\rangle$ by measuring its decay (with the rate being Γ) into state $|g\rangle$. The Hamiltonian describing such a simplest model in real space can be written as ($\hbar = 1$) [34–37]

$$\begin{aligned} H_1 = & \int dx a_R^\dagger(x)\left(-iv\frac{\partial}{\partial x}\right)a_R(x) + \int dx a_L^\dagger(x)\left(iv\frac{\partial}{\partial x}\right) \\ & \times a_L(x) + \int dx V\delta(x-x_0)[a_R(x)\sigma^+ + a_R^\dagger(x)\sigma^-] \\ & + \int dx V\delta(x-x_0)[a_L(x)\sigma^+ + a_L^\dagger(x)\sigma^-] \\ & + (\omega_0 - i\Gamma)\sigma^+\sigma^-. \end{aligned} \tag{1}$$

Here, $a_{L/R}^\dagger(x)$ and $a_{L/R}(x)$ represent the creation and annihilation operators of single photons propagating along the left and right directions, respectively. v is the group velocity of the traveling-wave photon, and V is the coupling strength between the photon and the atom. The raising (lowering) operator σ^+ (σ^-) reads $\sigma^+ = |1\rangle\langle 0|$ ($\sigma^- = |0\rangle\langle 1|$). ω_0 represents the transition frequency between the atomic state $|0\rangle$ and the excited one $|1\rangle$, and Γ is the rate of state $|1\rangle$ decaying into the readout state $|g\rangle$ for the measurement of the population of the atomic state $|1\rangle$.

Assuming that the atom is initially in state $|0\rangle$ and the traveling-wave photon is input from the left side of the waveguide and output at the right one, the generic wave function of the system can be expressed as [36]

$$\begin{aligned} |\psi_1(x,t)\rangle = & \int dx[\phi_{R,1}(x)a_R^\dagger(x) + \phi_{L,1}(x)a_L^\dagger(x)]|\varnothing\rangle \\ & + A_e\sigma^+|\varnothing\rangle, \end{aligned} \tag{2}$$

where $|\varnothing\rangle$ is the ground state of the system, i.e., the atom stays in state $|0\rangle$ and there is no photon in the waveguide. $\phi_{L,1/R,1}(x)$ and A_e denote the probabilistic amplitudes of a photon propagating along the left and right directions in the waveguide and excitation of the atom, respectively. Substituting this generic wave function into the time-dependent Schrödinger equation $i\partial_t|\psi_1(x,t)\rangle = H_1|\psi_1(x,t)\rangle$, we can get the time-independent Schrödinger equation

$$H_1|\psi_1(x)\rangle = \omega|\psi_1(x)\rangle. \tag{3}$$

The probabilistic amplitudes of a photon propagating along the right and left directions can be further expressed as [37]

$$\begin{aligned} \phi_{R,1}(x) &= e^{ikx}[\theta(-x+x_1) + t_1\theta(x+x_1)], \\ \phi_{L,1}(x) &= e^{-ikx}r_1\theta(-x+x_1), \end{aligned} \tag{4}$$

where t_1 and r_1 represent the transmitted and reflected probability amplitudes of the photon, respectively. k is the wave vector of the photon, and $\theta(x)$ is a step function. Without loss of generality, we set $x_1 = 0$. Substituting Eq. (4) into Eq. (3), we get

$$t_1 = \frac{\Delta + i\Gamma}{\Delta + i(\gamma+\Gamma)}, \quad r_1 = \frac{-i\gamma}{\Delta + i(\gamma+\Gamma)}, \tag{5}$$

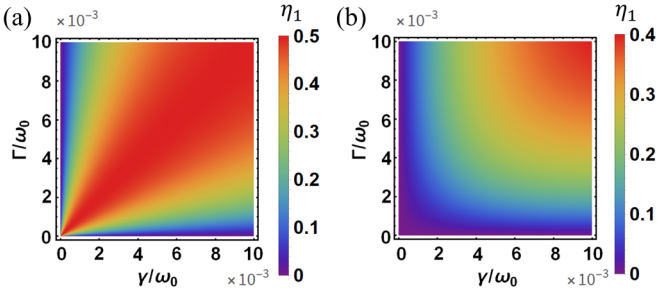

FIG. 2. The efficiency (absorption efficiency) η_1 (of a traveling-wave photon detected by a single three-level quantum detector) versus the effective detector-photon coupling strength γ and the decay rate Γ of the detector for (a) $\Delta = 0$ and (b) $\Delta = 0.01\omega_0$.

where $\Delta = \omega - \omega_0$ and $\gamma = V^2/v$ are the detuning and the effective coupling strength between the incident photon and the atom. Obviously, due to the existence of the decay Γ of the excited state $|1\rangle$, the detection efficiency of the photon can be expressed as [34]

$$\eta_1 = 1 - |t_1|^2 - |r_1|^2 = \frac{2\gamma\Gamma}{\Delta^2 + (\gamma + \Gamma)^2}. \tag{6}$$

Equation (6) indicates that η_1 is related to the controllable parameters Δ, γ, and Γ. However, as shown in Fig. 2, the maximal efficiency of the photon being detected by such an atomic detector is 50%, no matter how we adjust the relevant parameters [14,26]. This refers to the so-called photon absorption saturation of a single atom due to the natural impedance mismatch.

B. Single-photon detection with two interacting atoms

Given that the detection efficiency obtained using a single atomic detector cannot surpass 50%, we now discuss whether certain composite systems can be utilized to surpass such a limit. First, let us consider the detector configuration shown in Fig. 3, where two interacting three-level atoms serve as a single-photon detector. As the distance between the two neighboring interacting atoms is still significantly less than the wavelength of the microwave photon, two three-level atoms can still be regarded as a detector system located at $x_1 = 0$. Under the rotating-wave approximation, the Hamiltonian for

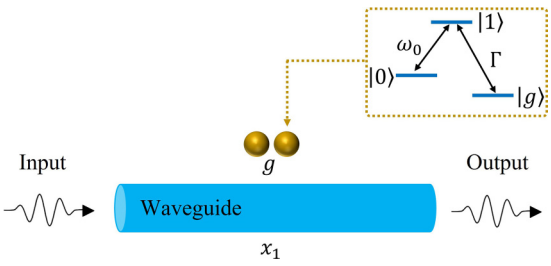

FIG. 3. Schematic diagram of a waveguide single photon scattered by single detectors located at x_1 consisting of two atoms with an interaction strength of g.

the present configuration can be expressed as [38,39]

$$\begin{aligned} H_2 = &\int dx a_R^\dagger(x)\left(-iv\frac{\partial}{\partial x}\right)a_R(x) + \int dx a_L^\dagger(x)\left(iv\frac{\partial}{\partial x}\right) \\ &\times a_L(x) + \sum_{j=1,2}\int dx V_j\delta(x)\{[\sigma_j^+ c_R(x) + \text{H.c.}] \\ &+ [\sigma_j^+ c_R(x) + \text{H.c.}]\} + \sum_{j=1}^{2}(\omega_i - i\Gamma_j)|1\rangle_j\langle 1|_j \\ &+ g(\sigma_1^+\sigma_2^- + \text{H.c.}). \end{aligned} \tag{7}$$

Here, $\sigma_j^+ = |1\rangle_j\langle 0|_j$ and $\sigma_j^- = |0\rangle_j\langle 1|_j$ are the jth atomic raising and lowering ladder operators. ω_j is the jth atomic transition frequency between states $|0_j\rangle$ and $|1_j\rangle$, and Γ_j is the decay rate of state $|1_j\rangle$. V_j is the coupling strength between the photon and the jth atom. g is the coupling strength between the two atoms.

Similarly, we assume that the atoms are initially prepared at state $|00\rangle$ and the microwave photon (with frequency ω) is input from the left. The generic wave function of the present system can be expressed as [39]

$$\begin{aligned} |\psi_c(x,t)\rangle = &\int dx\left[\phi_{R,c}(x)a_R^\dagger(x) + \phi_{L,c}(x)a_L^\dagger(x)\right]|\varnothing\rangle \\ &+ \sum_{j=1}^{2} A_{e,j}\sigma_j^+|\varnothing\rangle, \end{aligned} \tag{8}$$

where $A_{e,j}$ stands for the probabilistic amplitudes of the jth atom being excited into state $|1_j\rangle$ and $\phi_{L,c/R,c}(x)$ are the probabilistic amplitudes of the photon propagating along the left and right directions, respectively. Substituting Eqs. (7) and (8) into the time-independent Schrödinger equation (3) with the Hamiltonian H_1 replaced by the Hamiltonian H_2, we can obtain

$$\begin{aligned} &-iv\frac{\partial\phi_{R,c}(x)}{\partial x} + V_1A_1\delta(x) + V_2A_2\delta(x) \\ &\quad = \omega\phi_{R,c}(x), \end{aligned} \tag{9a}$$

$$\begin{aligned} &iv\frac{\partial\phi_{L,c}(x)}{\partial x} + V_1A_1\delta(x) + V_2A_2\delta(x) \\ &\quad = \omega\phi_{L,c}(x), \end{aligned} \tag{9b}$$

$$\begin{aligned} &(\omega_1 - i\Gamma_1)A_{e,1} + V_1[\phi_{L,c}(x) + \phi_{R,c}(x)] + gA_{e,2} \\ &\quad = \omega A_{e,1}, \end{aligned} \tag{9c}$$

$$\begin{aligned} &(\omega_2 - i\Gamma_2)A_{e,2} + V_2[\phi_{L,c}(x) + \phi_{R,c}(x)] + gA_{e,1} \\ &\quad = \omega A_{e,2}. \end{aligned} \tag{9d}$$

Again, the probability amplitude of the photon transported along the left and right directions can be expressed as

$$\begin{aligned} \phi_{R,c}(x) &= e^{ikx}[\theta(-x + x_1) + t_2\theta(x + x_1)], \\ \phi_{L,c}(x) &= e^{-ikx}r_2\theta(-x + x_1). \end{aligned} \tag{10}$$

Substituting Eq. (10) into Eq. (9), we have

$$t_2 = 1 - \frac{i[\gamma_1(\omega-\omega_2+i\Gamma_2)+\gamma_2(\omega-\omega_1+i\Gamma_1)+2g\sqrt{\gamma_1\gamma_2}]}{(\omega-\omega_1+i\Gamma_1+i\gamma_1)(\omega-\omega_2+i\Gamma_2+i\gamma_2)-(g-i\sqrt{\gamma_1\gamma_2})^2}, \tag{11a}$$

$$r_2 = \frac{-i[\gamma_1(\omega-\omega_2+i\Gamma_2)+\gamma_2(\omega-\omega_1+i\Gamma_1)+2g\sqrt{\gamma_1\gamma_2}]}{(\omega-\omega_1+i\Gamma_1+i\gamma_1)(\omega-\omega_2+i\Gamma_2+i\gamma_2)-(g-i\sqrt{\gamma_1\gamma_2})^2}, \tag{11b}$$

with $\Delta_{1,2} = \omega - \omega_{1,2}$ and $\gamma_{1,2} = V_{1,2}^2/v$, respectively. As a consequence, the efficiency of a traveling-wave photon being detected by such a two-atom detector can be calculated as $\eta_c = 1 - |t_2|^2 - |r_2|^2$.

Figure 4(a) shows how the detection efficiency η_c depends on the coupling strength g between the two atoms for the typical parameters $\gamma_1 = \gamma_2 = 0.005\omega_0$ and $\Gamma_1 = \Gamma_2 = 0.01\omega_0$. It is seen that, with the increase of the coupling strength g, the maximum detection efficiency point (corresponding to the resonance absorption of the photon) is shifted to the right. Moreover, Fig. 4(b) shows how the asymmetric features of the two atoms interacting with the photon expand the parameter regime to achieve the limit detection probability for the given coupling strength between the atoms. Although the upper limit of 50% detection efficiency still cannot be surpassed for two-interacting-atom detectors, the numerical results imply that the asymmetry of the atomic detectors could be utilized to change the detection efficiency of a single traveling-wave photon.

III. NONRECIPROCITY-ORGANIZED ATOMIC DETECTORS FOR HIGH-EFFICIENCY SINGLE-PHOTON DETECTION

Now, we discuss how to realize high-efficiency single-photon detection by using asymmetric atomic detectors. Simply, these asymmetries can be generated by using a series of individual atomic detectors with different parameters, including the detuning, the decay rates of the atomic excited states, and the distance between two detectors. Physically, these asymmetries lead to the nonreciprocity of the photon traveling along different directions through the detector array, and thus, the relevant transmitted and reflected probabilities of the itinerant photon are dependent on its incident directions. To investigate the transport property of a single microwave photon scattered by a series of atomic detectors, we introduce the relevant scattering matrix as follows. As illustrated in Fig. 5, when a single photon in the waveguide is scattered by a single two-level atom located at x_j, the left region of the atom exhibits both incident and reflected waves, while the right side of the atom has just the transmitted wave. Therefore, the scattering matrix $\mathbf{M}_j$ of the jth atomic detector can be defined as

$$\begin{pmatrix} t_j \\ 0 \end{pmatrix} = \mathbf{M}_j \begin{pmatrix} 1 \\ r_j \end{pmatrix}, \quad \begin{pmatrix} r_j \\ 1 \end{pmatrix} = \mathbf{M}_j \begin{pmatrix} 0 \\ t_j \end{pmatrix}.$$

According to Eq. (5), we get the scattering matrix

$$\mathbf{M}_j = \begin{pmatrix} \frac{t_j^2 - r_j^2}{t_j} & \frac{r_j}{t_j} \\ -\frac{r_j}{t_j} & \frac{1}{t_j} \end{pmatrix} = \begin{pmatrix} \frac{\Delta_j - i\gamma_j}{\Delta_j} & \frac{-i\gamma_j}{\Delta_j} \\ \frac{i\gamma_j}{\Delta_j} & \frac{\Delta_j + i\gamma_j}{\Delta_j} \end{pmatrix} \tag{12}$$

for the jth atomic detector, where

$$t_j = \frac{\Delta_j + i\Gamma_j}{\Delta_j + i(\gamma_j + \Gamma_j)}, \quad r_j = \frac{-i\gamma_j}{\Delta_j + i(\gamma_j + \Gamma_j)}, \tag{13}$$

and $\Delta_j = \omega - \omega_j$. Consequently, after sequential scatterings of N noninteracting atomic detectors, the probability amplitudes of the single-photon transmission and reflection can be written as [40–42]

$$\begin{pmatrix} \widetilde{t}_N \\ 0 \end{pmatrix} = \begin{pmatrix} e^{-i[\phi_1(x)+\phi_2(x)+\cdots\phi_{N-1}(x)]} & 0 \\ 0 & 1 \end{pmatrix} \widetilde{\mathbf{M}}_N \begin{pmatrix} 1 \\ \widetilde{r}_N \end{pmatrix}, \tag{14}$$

with

$$\widetilde{\mathbf{M}}_N = \mathbf{M}_1 \varphi(x_2 - x_1) \mathbf{M}_2 \varphi(x_3 - x_2) \cdots \mathbf{M}_N. \tag{15}$$

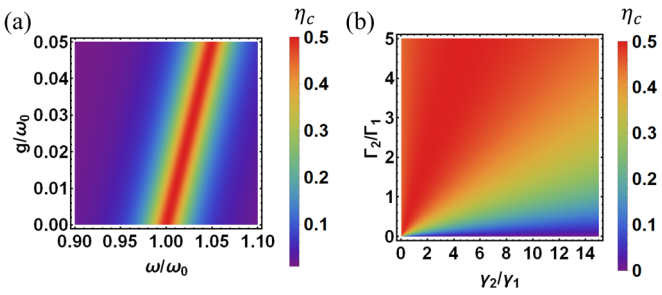

FIG. 4. The detection efficiency η_c (absorption efficiency) of a traveling-wave photon versus (a) the coupling strength g between the two detectors and frequency ω of the incident photon for $\gamma_1 = \gamma_2 = 0.005\omega_0$ and $\Gamma_1 = \Gamma_2 = 0.01\omega_0$ and (b) the ratio of the effective coupling strength γ_2/γ_1 and the ratio of the decay rate Γ_2/Γ_1 of the detectors for $g = 0.001\omega_0$, $\Delta_1 = \Delta_2 = 0$, $\gamma_1 = 0.005\omega_0$, and $\Gamma_1 = 0.01\omega_0$.

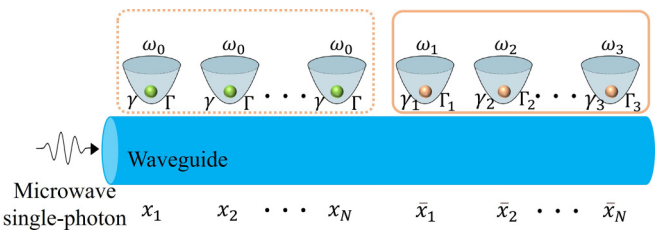

FIG. 5. Detector array for single-photon detection, where the green dot array (in the dotted box) refers to symmetrically arranged detectors (with the same excited frequency ω_0 and decay rate Γ of the atoms and also the same photon-atom coupling γ) and the gold dot array (in the solid box) is the nonreciprocity-organized atomic detectors (with different excited frequencies ω_j and decay rates γ_j of the atoms and also different photon-atom coupling strengths Γ_j). $x_1, x_2, \ldots, x_N$ and $\bar{x}_1, \bar{x}_2, \ldots, \bar{x}_N$ are the locations of the individual detectors.

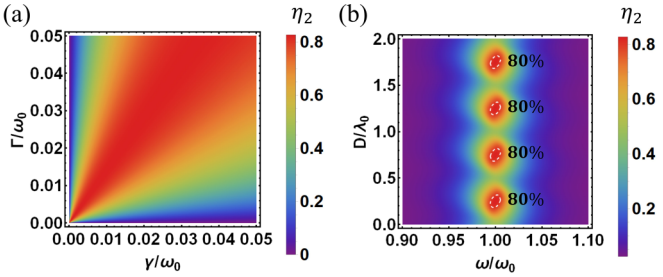

FIG. 6. The detection efficiency η_2 implemented by using two detectors arranged symmetrically versus (a) the detector-photon effective coupling strength γ and the decay rate Γ of the excited state of the detector for $\Delta = 0$ and $D = \lambda_0/4$ and (b) the ratio D/λ_0 and frequency ω of the incident photon for $\gamma_1 = \gamma_2 = 0.007\omega_0$ and $\Gamma_1 = \Gamma_2 = 0.01\omega_0$.

Here,

$$\varphi(x_{j+1} - x_j) = \begin{pmatrix} e^{i\phi_j(x)} & 0 \\ 0 & e^{-i\phi_j(x)} \end{pmatrix} \tag{16}$$

is the matrix of the free transport through distance $D_j = x_{j+1} - x_j$ (between two nearest-neighbor detectors), and thus,

$$\phi_j(x) = kn(x_{j+1} - x_j) = 2\pi n D_j/\lambda \tag{17}$$

is the relevant phase shift acquired by the free transport of the traveling-wave photon through distance D_j. Above, n is the refractive index (which is here set to $n = 1$ for simplicity) of the waveguide, and λ is the wavelength of the traveling-wave photon. Therefore, the efficiency of the traveling-wave photon detected successively by an N-detector array can be calculated as [14]

$$\eta_N = 1 - |\widetilde{t}_N|^2 - |\widetilde{r}_N|^2. \tag{18}$$

This implies that the detection efficiency of the photon can be engineered by properly arranging the detectors to generate certain arrays with as few individual detectors as possible. It is seen that ideal detection refers to complete impedance matching without any reflection and transmission.

A. Efficiency of the photon detected sequentially by the symmetrically-arranged detectors

First, let us discuss how many symmetrically arranged detectors are sufficient to realize the deterministic detection of a traveling-wave photon. Here, the symmetric arrangement of the detectors means that the N individual atomic detectors generate a periodic array in which each of the detectors possesses the same physical parameters, i.e., $\omega_j = \omega_0$, $\gamma_j = \gamma$, $\phi_j = \phi$, and $\Gamma_j = \Gamma$.

Simply, if the array contains two detectors, we have

$$\widetilde{t}_2 = \frac{\beta^2}{(\beta+1) - e^{2i\phi}}, \tag{19a}$$

$$\widetilde{r}_2 = \frac{\beta + 1 + (\beta-1)e^{2i\phi}}{e^{2i\phi} - (\beta+1)^2}, \tag{19b}$$

with $\beta = [i\Gamma + (\omega - \omega_0)]/i\gamma$. The corresponding detection efficiencies are shown in Fig. 6 for $\gamma = 0.007\omega_0$ and $\Gamma = 0.01\omega_0$. Figure 6(a) shows that the efficiency η_2 of the photon being detected by the symmetrically arranged array with $N = 2$ identical detectors can be maximized to ∼82.8% for $\Delta = 0$ and $D = \lambda_0/4$. Figure 6(b) shows that the detection efficiency η_2 can be enhanced by adjusting the distance D between the two detectors. In particular, the detection efficiency maximizes to ∼82.8% for $D = (2m+1)\lambda_0/4 (m = 0, 1, 2, \ldots)$.

One can easily check that the detection efficiency of the photon cannot be linearly increased by adding to the number of detectors in such a symmetrically arranged array. For example, if the array contains $N = 3$ detectors, we get

$$\widetilde{t}_3 = \frac{\beta^3}{(\beta+1)^3 - 2(\beta+1)e^{2i\phi} - (\beta-1)e^{4i\phi}}, \tag{20a}$$

$$\widetilde{r}_3 = \frac{(1-e^{2i\phi})^2 + 2\beta(e^{4i\phi}-1) - \beta^2(1+e^{2i\phi}+e^{4i\phi})}{3\beta^2 + \beta^3 + (e^{2i\phi}-1)^2 + \beta(3-2e^{2i\phi}-e^{4i\phi})}. \tag{20b}$$

We can easily check that the maximized detection efficiency η_3 can reach only ∼87.82%, which is not a major improvement compared with that realized by using two identical detectors. Roughly, for detection efficiency tending to 100%, the number of identical detectors in such a symmetric array is estimated to be ∼20 [14]. Therefore, enhancing the probability of the photon being detected sequentially by adding to the number of identical detectors in such a symmetric array is practically undesirable.

B. Two nonreciprocity-organized detectors for high-efficiency single-photon detection

Below, we discuss how to significantly enhance the detection efficiency of a single itinerant photon by alternatively organizing a few atomic detectors as an asymmetric array with controllable nonreciprocity. We show that, even with the simplest nonreciprocity-organized array with two atomic detectors, the detection efficiency of the photon can be significantly improved compared with those obtained by either coupling them as a composite system (as discussed in Sec. II B) or arranging them in a symmetric array (as demonstrated in Sec. III A).

In fact, for an array with just two atomic detectors arranged asymmetrically with an interval $D_1 = \bar{x}_2 - \bar{x}_1$, the transmitted and reflected probabilistic amplitudes can be calculated as

$$\bar{t}_2^{L\to R} = \frac{\beta_1\beta_2}{(\beta_1+1)(\beta_2+1) - e^{2i\phi_1(x)}}, \tag{21a}$$

$$\bar{r}_2^{L\to R} = \frac{\beta_1 + 1 + (\beta_2-1)e^{2i\phi_1(x)}}{e^{2i\phi_1(x)} - (\beta_1+1)(\beta_2+1)} \tag{21b}$$

if the traveling-wave photons are input from the left side and transmit through the detector array, where $\beta_j = [i\Gamma_j + (\omega - \omega_j)]/i\gamma_j$. In this case, the detection efficiency of such a right-traveling photon can be expressed as [14]

$$\bar{\eta}_2^{L\to R} = 1 - \left|\bar{t}_2^{L\to R}\right|^2 - \left|\bar{r}_2^{L\to R}\right|^2. \tag{22}$$

Obviously, the asymmetry of such a simple array can be generated if the condition $\gamma_1 \neq \gamma_2$ or $\Gamma_1 \neq \Gamma_2$ is satisfied. Specifically, as shown in Fig. 7, the reachable detection efficiency $\bar{\eta}_2^{L\to R}$ is maximized to ∼99.18% by optimizing the asymmetric parameters, such as γ_2/γ_1 for $\Gamma_1 = \Gamma_2 = 0.01\omega_0$, $\gamma_1 = 0.05\omega_0$, and $D_1 = \lambda_0/4$; Γ_2/Γ_1 for

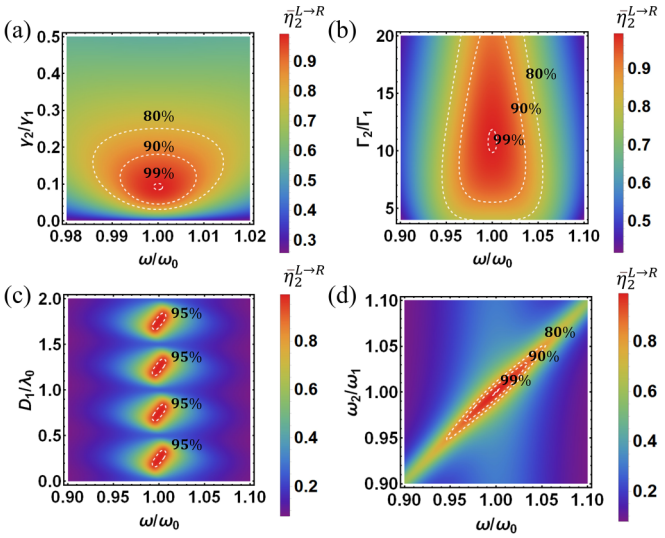

FIG. 7. Efficiency of a single photon detected by an asymmetrically arranged array with two detectors versus (a) γ_2/γ_1, with $\Gamma_1 = \Gamma_2 = 0.01\omega_0$, $\gamma_1 = 0.05\omega_0$, and $D_1 = \lambda_0/4$; (b) Γ_2/Γ_1, with $\gamma_1 = \gamma_2 = 0.05\omega_0$, $\Gamma_1 = 0.01\omega_0$, and $D_1 = \lambda_0/4$; (c) the distance between two detectors D_1/λ_0, with $\gamma_1 = 0.05\omega_0$, $\gamma_2 = 0.093\gamma_1$, $\Gamma_1 = \Gamma_2 = 0.01\omega_0$, and $\omega_1 = \omega_2 = \omega_0$; and (d) ω_2/ω_1, with $D_1 = \lambda_0/4$, $\gamma_1 = 0.05\omega_0$, $\gamma_2 = 0.093\gamma_1$, and $\Gamma_1 = \Gamma_2 = 0.01\omega_0$.

$\gamma_1 = \gamma_2 = 0.05\omega_0$, $\Gamma_1 = 0.01\omega_0$, and $D_1 = \lambda_0/4$; and also the distance D_1 between the two detectors for $\gamma_1 = 0.05\omega_0$, $\gamma_2 = 0.093\gamma_1$, $\Gamma_1 = \Gamma_2 = 0.01\omega_0$, and $\omega_1 = \omega_2 = \omega_0$, etc. Obviously, compared with the symmetrically arranged array with two single-photon detectors, the maximal detection efficiency of the photon can be significantly enhanced. Certainly, these asymmetries originate from the difference in at least one of the physical parameters of the detectors, typically the decay rate Γ_j of the excited state or the photon-detector coupling strength γ_j. Furthermore, the distance D_1 between two detectors influences the relevant quantum interference effect of the photon and thus its detection efficiency.

The significantly enhanced detection efficiency demonstrated above benefits from the asymmetry organization of the detectors. Physically, such asymmetry implies that the relevant array is a nonreciprocal device; i.e., the transmitted probability of the traveling-wave photon being scattered by the device is dependent on its transporting directions, although it transports along the same waveguide. To check this property, let us calculate the transmitted or reflected probability of the traveling-wave photon being scattered by such an asymmetric array. Obviously, replacing $\beta_{1,2}$ by $\beta_{2,1}$ in Eq. (21), we get

$$\bar{t}_2^{R\to L} = \frac{\beta_1\beta_2}{(\beta_1+1)(\beta_2+1) - e^{-2i\phi_1(x)}}, \tag{23a}$$

$$\bar{r}_2^{R\to L} = \frac{\beta_2 + 1 + (\beta_1 - 1)e^{-2i\phi_1(x)}}{e^{-2i\phi_1(x)} - (\beta_1+1)(\beta_2+1)} \tag{23b}$$

for the transmitted or reflected probabilistic amplitude of the photon transported from the right to left being scattered by such an asymmetric two-detector array.

As shown in Fig. 8, when waveguide photons transmit in two opposite directions through two asymmetrically organized detectors, they exhibit different transmission characteristics. Especially at the resonance frequency point ω_0, the transmission probabilities of photons transmitted in opposite directions are the same (i.e., $|\bar{t}_2^{L\to R}|^2 = |\bar{t}_2^{R\to L}|^2 \approx 0.0081$), and the reflection probabilities are different (i.e., $|\bar{r}_2^{L\to R}|^2 \approx 0.0001$, $|\bar{r}_2^{R\to L}|^2 \approx 0.6829$). Here, time-reversal symmetry is broken by adjusting the photon-detector coupling strength γ_j or the dissipation rate Γ_j of the atoms in the detector array [30]. Correspondingly, the efficiency of the left-traveling photon being detected by such an asymmetrically organized two-detector array can be presented as

$$\bar{\eta}_2^{R\to L} = 1 - \left|\bar{t}_2^{R\to L}\right|^2 - \left|\bar{r}_2^{R\to L}\right|^2. \tag{24}$$

Phenomenologically, one can introduce a nonreciprocal coefficient

$$\kappa_2 = \left| \frac{\left|\bar{r}_2^{L\to R}\right|^2 - \left|\bar{r}_2^{R\to L}\right|^2}{\left|\bar{r}_2^{L\to R}\right|^2 + \left|\bar{r}_2^{R\to L}\right|^2} \right|, \tag{25}$$

to describe the asymmetry effect; i.e., $\kappa = 0$ and $\kappa = 1$ refer to the reciprocity and the maximal nonreciprocity, respectively. Figure 9 shows that the stronger nonreciprocity corresponds to the maximal detection efficiency. Typically,

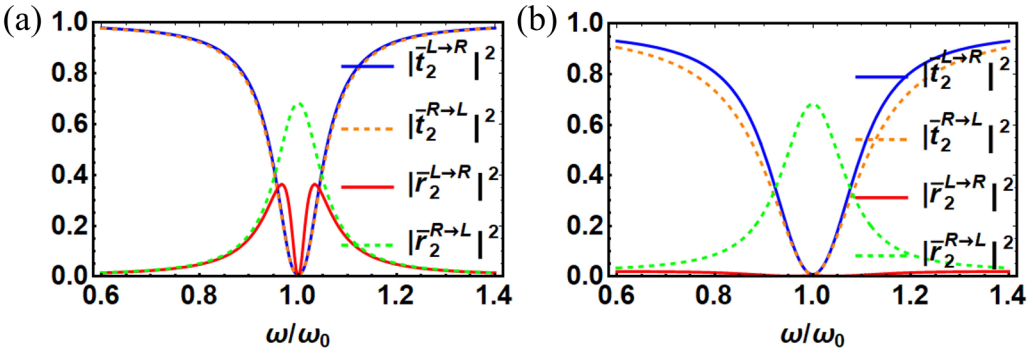

FIG. 8. The transmission probability $|\bar{t}_2^{L\to R}|^2(|\bar{t}_2^{R\to L}|^2)$ and the reflection probability $|\bar{r}_2^{L\to R}|^2(|\bar{r}_2^{R\to L}|^2)$ for the left- and right-traveling photons scattered by two asymmetrically organized detectors. (a) The effective coupling strengths of the two atoms are set as $\gamma_2 = 0.093\gamma_1$ and $\Gamma_1 = \Gamma_2$. (b) The dissipation rates of two atoms in the detector arrays are set as $\Gamma_2 = 10\Gamma_1$ and $\gamma_1 = \gamma_2$. Here, the other relevant parameters are set as $D_1 = \lambda_0/4$, $\Gamma_1 = 0.01\omega_0$, $\gamma_1 = 0.05\omega_0$, and $\omega_1 = \omega_2 = \omega_0$.

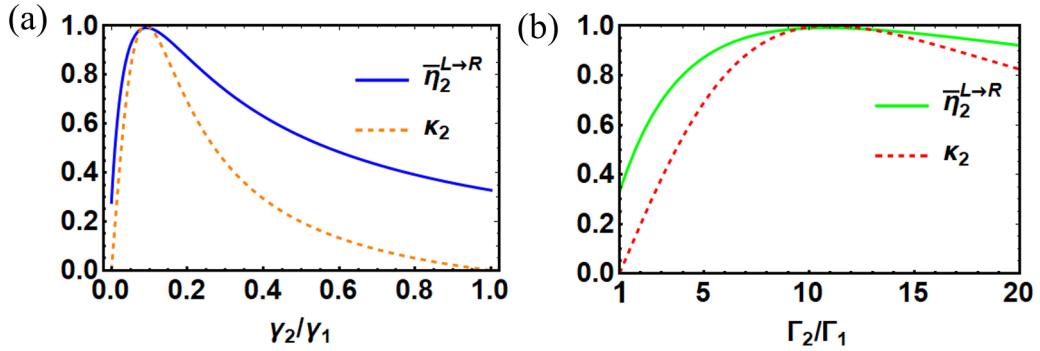

FIG. 9. The detection efficiency of a single photon $\bar{\eta}_2^{L\to R}$ and the nonreciprocal coefficient κ_2 versus (a) the ratio γ_2/γ_1 of the effective coupling strength, with $\Gamma_1 = \Gamma_2 = 0.01\omega_0$ and $\gamma_1 = 0.05\omega_0$, and (b) the ratio γ_2/γ_1 of the decay rate, with $\gamma_1 = \gamma_2 = 0.05\omega_0$ and $\Gamma_1 = 0.01\omega_0$. The relevant parameters are chosen as $D_1 = \lambda_0/4$ and $\omega_1 = \omega_2 = \omega = \omega_0$.

the maximal detection efficiency can reach 99.18% if the nonreciprocal coefficient is $\kappa_2 = 1$.

C. Ideal single-photon detection with a nonreciprocal array by the complete impedance matching

In the above investigation, the detection efficiency of photons in the two-detector nonreciprocally arranged array is significantly enhanced compared to the reciprocal arrangement. However, the detection efficiency of waveguide photons still cannot approach 100%. Inspired by the fact that photon detection efficiency can be improved by increasing the number of symmetrically arranged detectors [14,26], we discuss specifically the idea that photon detection efficiency can be further improved by adjusting the relevant parameters in a nonreciprocal array with three nonidentical detectors and then argue that detection efficiency approaching 100% could be achieved if the number of detectors could be further increased.

According to Eq. (14), the transmission and reflection probability amplitudes of traveling wave photons propagating from left to right through three asymmetrically arranged detectors with intervals of D_1 and D_2 can be calculated as

$$\bar{t}_3^{L\to R} = \frac{\beta_1\beta_2\beta_3}{-e^{2i\phi_2(x)}[\beta_1+1+e^{2i\phi_1(x)}(\beta_2-1)]+(\beta_3+1)[(\beta_1+1)(\beta_2+1)-e^{2i\phi_1(x)}]}, \tag{26a}$$

$$\bar{r}_3^{L\to R} = \frac{(\beta_1+1)(\beta_2+1)-e^{2i\phi_1(x)}+e^{2i\phi_2(x)}(\beta_3-1)[\beta_1+1+e^{2i\phi_1(x)}(\beta_2-1)]}{e^{2i\phi_2(x)}[\beta_1+1+e^{2i\phi_1(x)}(\beta_2-1)]+(\beta_3+1)[e^{2i\phi_1(x)}-(\beta_1+1)(\beta_2+1)]}. \tag{26b}$$

In this case, the detection efficiency of such a right-traveling photon can be expressed as [14]

$$\bar{\eta}_3^{L\to R} = 1 - \left|\bar{t}_3^{L\to R}\right|^2 - \left|\bar{r}_3^{L\to R}\right|^2. \tag{27}$$

Above, we discussed the influence of the detector parameters, γ, Γ, and D_1/λ_0, on the detection efficiency of a two-detector nonreciprocal array. Below, we investigate in particular how the distances D_1 and D_2 influence the detection efficiency in such an asymmetrically arranged three-detector array. Figure 10 shows the achievable high-efficiency detection (e.g., $\bar{\eta}_3^{L\to R} > 99.9\%$, inside the white dotted lines) of a photon with frequency ω_0 versus the distance $D_2 = (2m+1)\lambda_0/4 (m = 0, 1, 2, \dots)$. Here, the other parameters are set as $D_1 = \lambda_0/4$, $\gamma_1 = \gamma_2 = 0.05\omega_0$, $\gamma_3 = 0.093\gamma_1$, $\Gamma_1 = \Gamma_2 = \Gamma_3 = 0.01\omega_0$, and $\omega_1 = \omega_2 = \omega_3 = \omega_0$. It is seen that the detection efficiency can reach 99.97% for $D_1 = D_2 = (2m+1)\lambda_0/4 (m = 0, 1, 2, \dots)$.

As shown in Fig. 11, for the asymmetrically organized three-detector array, different transmission characteristics can be observed if the photons are input from opposite directions. This implies that the array is really nonreciprocal [30]. Correspondingly, the nonreciprocal coefficient can be calculated as

$$\kappa_3 = \left|\frac{\left|\bar{r}_3^{L\to R}\right|^2 - \left|\bar{r}_3^{R\to L}\right|^2}{\left|\bar{r}_3^{L\to R}\right|^2 + \left|\bar{r}_3^{R\to L}\right|^2}\right|, \tag{28}$$

where the definition of $\bar{r}_3^{L\to R}$ is shown in the Appendix.

Indeed, impedance matching is an important technique to minimize reflections and thus maximize the power transfer by adjusting the input and output impedances of electrical components and circuits [43]. Physically, the ideal impedance match refers to the reflected coefficient of the incident waves approaching zero. This technique has already been utilized to implement microwave photon detection using qubit-resonator coupling [17,18]. In the present work, we have shown alternatively that, by employing the nonuniform parameters of the artificial atoms, the reflected probability of the incident single-photon microwave signal can be significantly lowered, thereby achieving the desired impedance matching. Furthermore, if the transmission probability of the incident single-photon microwave also approaches zero, then perfect absorption can be achieved. This can be clearly verified in Fig. 11, where both the transmission and reflection coefficients of the microwave photon approach zero and thus the incident photon is perfectly absorbed.

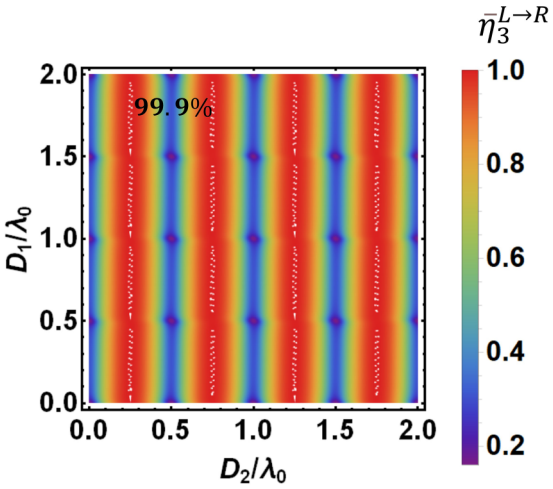

FIG. 10. The detection efficiency $\bar{\eta}_3^{L\to R}$ of the photon with a frequency of ω_0 versus the distances D_1 and D_2. The relevant parameters are chosen as $\Gamma_1 = \Gamma_2 = \Gamma_3 = 0.01\omega_0$, $\gamma_1 = \gamma_2 = 0.05\omega_0$, $\gamma_3 = 0.093\gamma_1$, and $\omega_1 = \omega_2 = \omega_3 = \omega_0$.

Phenomenologically, nonreciprocity of the wave propagation arises basically from the breaking of time-reversal symmetry, disrupting the equivalence of forward and backward wave transmissions [30]. In the present work, we have shown that the nonreciprocity cannot be realized by using a single atomic detector, and thus, the desired impedance match cannot be achieved. However, if a few atomic detectors with nonuniform parameters form a detector array (and thus break the time-reversal symmetry), the nonreciprocity can be obtained (see Fig. 11). As a consequence, the desired impedance match without the reflection of the single-photon microwave can be realized.

Specifically, we can see from Fig. 12 that the trends of the single-photon detection efficiency $\bar{\eta}_3^{L\to R}$ and nonreciprocal coefficient κ_3 are consistent; i.e., stronger nonreciprocity corresponds to higher detection efficiency. In particular, Fig. 12(a) verifies again that, when the distance $D_2 = \lambda_0/4$ is fixed, highly efficient single-photon detection for a photon with frequency ω_0 is sufficiently robust for the selection of the distance D_1. Therefore, with the choice of appropriate parameters, such as $D_1 = D_2 = \lambda_0/4$, the transmission probability and reflection probability of photons propagating from left to right are both zero. As a consequence, the detection efficiency of single photons can reach 99.97%. The perfect distances of the nonreciprocities, shown in Fig. 12, imply that quantum interference is also one of the origins of the nonreciprocity.

Interestingly, with such a nonreciprocal three-detector array, high-efficiency detection of single itinerant photons with other frequencies can still be achieved. As shown in Fig. 13, when the transition frequencies of the atoms are set as $\omega' = 0.9\omega_0, 1.1\omega_0, 1.2\omega_0$, the achievable values of $\bar{\eta}_3^{L\to R}$ are 99.38%, 99.38%, and 97.58%, respectively. The corresponding nonreciprocal coefficients κ_3 are 0.982, 0.982, and 0.931 for $\Gamma_1 = \Gamma_2 = \Gamma_3 = 0.01\omega_0$, $\gamma_1 = \gamma_2 = 0.05\omega_0$, $\gamma_3 = 0.093\gamma_1$, and $D_1 = D_2 = \lambda_0/4$.

Given that the detection efficiencies of the nonreciprocal arrays with two and three nonidentical detectors demonstrated above have approached 100%, we argue that the implementation of ideal detection of a single photon is desirable once the number of detectors can be further increased.

IV. A FEASIBLE NONRECIPROCAL DETECTOR ARRAY TO IMPLEMENT HIGH-EFFICIENCY DETECTION OF A SINGLE MICROWAVE ITINERANT PHOTON

Experimentally, various solid-state qubits, such as superconducting transmon and Xmon qubits [44,45], and semiconductor quantum-dot qubits [46] can be utilized to generate the proposed nonreciprocal atomic detector array to implement the desired high-efficiency detection of a single itinerant microwave photon. Without loss of generality, Fig. 14 shows a feasible configuration by specifically using current-biased Josephson-junction (CBJJ) detectors [47]. Here, each of the artificial three-level atomic detectors is designed by capacitively. Here, each of the artificial three-level atomic detectors is capacitively coupled to the itinerant microwave photon, which is transported along a superconducting transmission line.

Initially, the CBJJ-based atomic detector is prepared in its zero-voltage state $|0\rangle$, i.e., the ground state of a "particle" trapped in a potential [14,26] $U_j(\delta) = -I_{c,j}\Phi_0(\cos\delta + I_{b,j}\delta/I_{c,j})/(2\pi)$. Here, $\Phi_0 = \pi\hbar/(2e)$ is the flux quanta, $\delta = 2\pi\Phi/\Phi_0$ is the gauge-invariant phase across the junction, and I_c is the critical current of the junction. The incident microwave photon (with frequency $\sim\omega_0$) excites the CBJJ into state $|1\rangle$, which is very unstable and thus will quickly tunnel into the voltage state $|g\rangle$. Therefore, if we probe the voltage response of the CBJJ detector, corresponding to state $|g\rangle$, the itinerant microwave photon can be detected. In fact, the rate of state $|1\rangle$ tunneling into state $|g\rangle$ is significantly larger than that of state $|0\rangle$, typically $\Gamma_{|1\rangle}/\Gamma_{|0\rangle} \sim 1000$ [26]. Therefore, we can confirm that the voltage state is due to the tunneling from state $|1\rangle$, rather than state $|0\rangle$. Importantly, given that the detection efficiency of a single CBJJ detector is very limited, three CBJJ detectors with controllable physical parameters, i.e., the eigenfrequencies, dissipation, effective detector-photon coupling strengths, and the interdetector distances, are arranged asymmetrically as a nonreciprocal detector array. The three detectors are connected to a common voltmeter for the readout of the response from any one of the detectors.

Certainly, the physical parameters of each of the CBJJ-based detectors can be properly set, and thus, the three detectors can be asymmetrically arranged as a nonreciprocal array. For example, the transition frequency ω_0 between states $|0\rangle$ and $|1\rangle$ can be controlled by properly setting the Josephson capacitance C_J, critical current I_c, biased dc current I_b, and thus the eigenfrequency of the bound states of the CBJJ Hamiltonian: $H_{\mathrm{CBJJ},j} = \frac{(2e)^2}{2C_{J,j}} + U_j(\delta)$. For example, if $I_c = 0.98\ \mu$A, $C_J = 0.9$ pF, and $I_b = 0.96I_c$ [16], then CBJJs exist in two bound states, $|0\rangle$ and $|1\rangle$, with $\omega_0 = 2\pi \times 4.84$ GHz [48]. The coupling strength V_j between the superconducting transmission line and the jth CBJJ can be determined as [26] $\hbar V_j = \frac{C_{g,j}}{C_{J,j}+C_{g,j}}\frac{e}{\alpha}\sqrt{\frac{\hbar\omega_{0,j}}{c}}$, where $C_{g,j}$ is the coupling capacitance and $\alpha_j^2 = E_{c,j}/\hbar\omega_{0,j}$ is experimentally designed. Here, $E_{c,j} = (2e)^2/2C_{J,j}$ is the junction charging energy, and c is

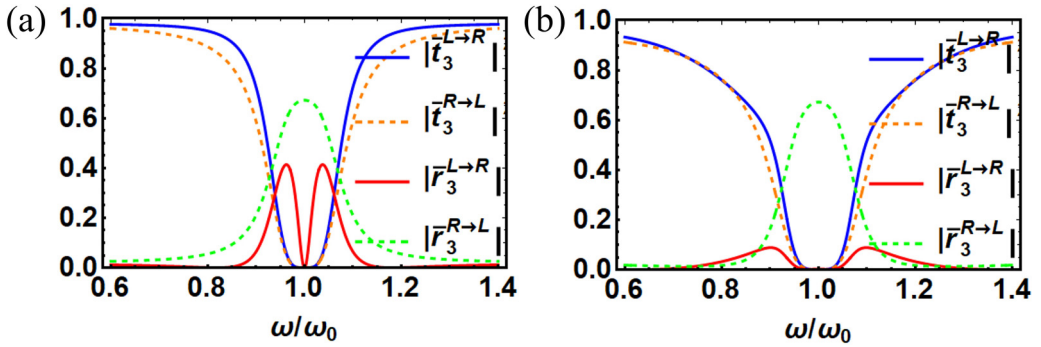

FIG. 11. The transmission probability $|\bar{t}_3^{L\to R}|^2$ ($|\bar{t}_3^{R\to L}|^2$) and the reflection probability $|\bar{r}_3^{L\to R}|^2$ ($|\bar{r}_3^{R\to L}|^2$) when the waveguide photons are transmitted from left to right (right to left) through the three asymmetrically organized detectors. (a) The effective coupling strengths for the first and third atoms are different in the detector arrays, where $\gamma_1 = \gamma_2$, $\gamma_3 = 0.093\gamma_1$, and $\Gamma_1 = \Gamma_2 = \Gamma_3$. (b) The decay rates of the first and third atoms are different in the detector arrays, where $\Gamma_1 = \Gamma_2$, $\Gamma_3 = 10\Gamma_1$, and $\gamma_1 = \gamma_2 = \gamma_3$. The other parameters are chosen as $\omega_1 = \omega_2 = \omega_3 = \omega_0$, $D_1 = D_2 = \lambda_0/4$, $\gamma_1 = 0.01\omega_0$, $\Gamma_1 = 0.05\omega_0$.

the capacitance per unit length of the transmission line. As a consequence, the effective coupling strength

$$\gamma_j = \frac{V_j^2}{v} = \left(\frac{C_{g,j}}{C_{g,j}+C_{J,j}}\right)^2 \frac{\omega_{01,j}e^2Z_0}{\hbar\alpha_j^2} \tag{29}$$

between the jth CBJJ-based detector and the photon, where $v = 1/\sqrt{lc} = 1/(cZ_0)$, with l being the inductance per unit length of the transmission line and Z_0 being the characteristic impedance of transmission line, is also designable. Furthermore, the dissipation rate [15]

$$\Gamma_j = \frac{\omega_{0,j}\pi[432\Delta U_j/(\hbar\omega_{0,j})]^{3/2}}{\sqrt{\pi}} \exp\left[-\frac{36\Delta U_j}{5\hbar\omega_{0,j}}\right] \tag{30}$$

is really controllable, as the barrier height $\Delta U_j = 4I_{c,j}\Phi_0/3\sqrt{2}\pi(1-I_{b,j}/I_{c,j})^{3/2}$ of the jth CBJJ is still adjustable. These controllable physical parameters of each of the CBJJ-based detectors suggest that the desired nonreciprocal array can be constructed by using three CBJJ-based detectors.

Specifically, in order to realize the detection of the microwave single photon at the frequency $\omega_{01} = 2\pi \times 4.84$ GHz, with the high-efficiency detection approaching 100%, the relevant parameters can be designated as $\Gamma_1 = \Gamma_2 = \Gamma_3 = 0.01\omega_{01}$, $\gamma_1 = \gamma_2 = 0.05\omega_{01}$, $\gamma_3 = 0.093\gamma_1$, and $D_1 = D_2 = \lambda_{01}/4$ by properly setting the capacitance parameters as $C_{g,1} = C_{g,2} = 1.9$ pF and $C_{g,3} = 0.23$ pF. Therefore, the desired nonreciprocal detector array generated by a few CBJJs for high-efficiency detection of a single microwave itinerant photon is feasible by engineering the relevant parameters of the detectors.

V. CONCLUSION

In summary, we demonstrated theoretically that a nonreciprocity array with a few detectors can be constructed to implement high-efficiency detection of a single microwave itinerant photon. Different from the reciprocity detector array, which usually requires more than 20 identical detectors arranged symmetrically to implement ∼100% detection efficiency, two or three detectors are sufficient to achieve the desired high-efficiency (approaching 100%) detection of a single microwave itinerant photon. The nonreciprocity can be achieved by properly adjusting the physical parameters of the detectors. The induced nonreciprocity of the array can be verified by measuring the transmitted and reflected probabilities of a photon incident from different directions. Physically, ideal detection efficiency practically refers to complete impedance matching, leading to the zero probability of the transmission and reflection of the incident photon.

It is noteworthy that, if the physical parameters of the detectors, such as the coupling strength between the detector

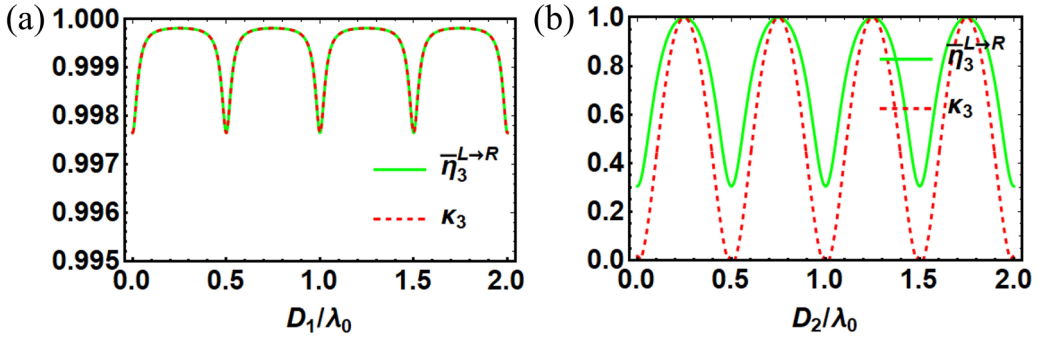

FIG. 12. The influence of the distances (D_1 and D_2) between two nearest-neighbor detectors on the photon with a frequency ω_0, detection efficiency $\bar{\eta}_3^{L\to R}$, and nonreciprocal coefficient κ_3, where (a) $D_2 = \lambda_0/4$ and (b) $D_1 = \lambda_0/4$. The other relevant parameters are chosen as $\Gamma_1 = \Gamma_2 = \Gamma_3 = 0.01\omega_0$, $\gamma_1 = \gamma_2 = 0.05\omega_0$, $\gamma_3 = 0.093\gamma_1$, and $\omega_1 = \omega_2 = \omega_3 = \omega_0$.

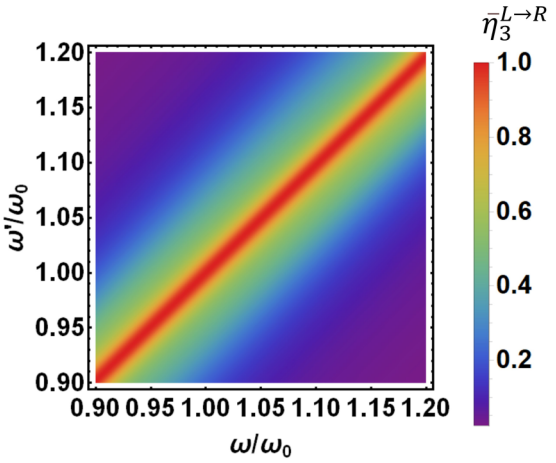

FIG. 13. Detection efficiency $\bar{\eta}_3^{L\to R}$ versus the detector eigenfrequency $\omega_1 = \omega_2 = \omega_3 = \omega'$ and the frequency ω of the incident microwave photon. The relevant parameters are set as $\Gamma_1 = \Gamma_2 = \Gamma_3 = 0.01\omega_0$, $\gamma_1 = \gamma_2 = 0.05\omega_0$, $\gamma_3 = 0.093\gamma_1$, and $D_1 = D_2 = \lambda_0/4$.

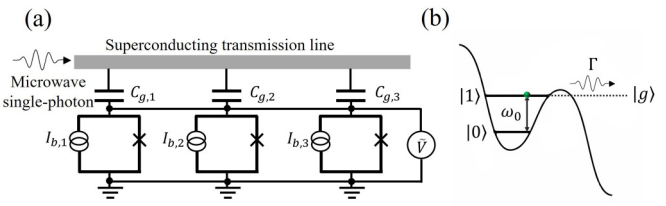

FIG. 14. (a) A nonreciprocal CBJJ-based array containing three asymmetrically arranged detectors for the high-efficiency detection of a single itinerant microwave photon transported along the capacitively coupled superconducting transmission line. Here, $C_{g,j}$ and $I_{b,j}$ ($j = 1, 2, 3$) denote the capacitance and the biased dc current of the jth CBJJ, respectively. $\widetilde{V}$ represents the voltmeter for the readout of the voltage response from any one of the detectors. (b) Detection principle of a single microwave photon using a CBJJ detector which is initially prepared at state $|0\rangle$ and can be excited to state $|1\rangle$ by the coupled microwave photon. State $|1\rangle$ will quickly tunnel into the voltage state $|g\rangle$ for the implementation of the single-photon detection.

and the photon, the decay rate of the excited state of the detector, and the transition frequency between the ground and excited states of the detector, are properly designed, the detection efficiency of a single microwave itinerant photon can be significantly improved. The feasibility of the proposal was demonstrated by the designing of a nonreciprocity array containing two or three CBJJ-based detectors. Because the techniques to fabricate these devices are well developed, we believe that the implementation of the detection of a single microwave itinerant photon with sufficiently high efficiency is feasible, in principle. Probably, a potential challenge of the proposal is that the experimental detection efficiency of a single atomic detector is still limited due to its practical imperfect absorptions; i.e., the signal cannot be detected even if the photon is absorbed. Therefore, if a single microwave photon is imperfectly absorbed by the former detector, it has no chance of being detected by the latter detectors. Therefore, the robustness of the present scheme is based on the higher detection efficiency of a single detector. With the higher detection efficiency of a single detector, a smaller number of detectors are required for the construction of a nonreciprocity detector array for ideal detection of a single microwave photon.

ACKNOWLEDGMENTS

This work was partially supported by the National Key Research and Development Program of China under Grant No. 2021YFA0718803 and by the National Natural Science Foundation under Grant No. 11974290.

APPENDIX

In this Appendix, we provide the transmission parameters for the traveling-wave photons incident from the right side of the detector array. Similarly, if the photon is incident from the right and then is sequentially scattered by N asymmetrically arranged detectors, we have

$$\begin{pmatrix} \bar{t}_N^{R\to L} \\ 0 \end{pmatrix} = \begin{pmatrix} e^{i[\phi_1(x)+\phi_2(x)+\cdots+\phi_{N-1}(x)]} & 0 \\ 0 & 1 \end{pmatrix} \mathbf{M}'_N \begin{pmatrix} 1 \\ \bar{r}_N^{R\to L} \end{pmatrix} \tag{A1}$$

and $\mathbf{S}'_N = \mathbf{M}_N \varphi(x_{N-1} - x_N)\mathbf{M}_{N-1}\varphi(x_{N-2} - x_{N-1}) \cdots \varphi(x_1 - x_2)\mathbf{M}_1$. Here, the phase shift matrix reads

$$\varphi(x_{j-1} - x_j) = \begin{pmatrix} e^{-i\phi_j(x)} & 0 \\ 0 & e^{i\phi_j(x)} \end{pmatrix}.$$

Specifically, for $N = 3$, we can easily get

$$\bar{t}_3^{R\to L} = \frac{\beta_1\beta_2\beta_3}{-e^{-2i\phi_2(x)}[\beta_1 + 1 + e^{-2i\phi_1(x)}(\beta_2 - 1)] + (\beta_3 + 1)[(\beta_1 + 1)(\beta_2 + 1) - e^{-2i\phi_1(x)}]}, \tag{A1a}$$

$$\bar{r}_3^{R\to L} = \frac{(\beta_1 - 1)(1 - \beta_2)e^{-2i[\phi_1(x)+\phi_2(x)]} + e^{-2i\phi_2(x)} - (\beta_3 + 1)[\beta_2 + 1 + e^{-2i\phi_1(x)}(\beta_1 - 1)]}{e^{-2i\phi_2(x)}[\beta_1 + 1 + e^{-2i\phi_1(x)}(\beta_2 - 1)] + (\beta_3 + 1)[e^{-2i\phi_1(x)} - (\beta_1 + 1)(\beta_2 + 1)]}. \tag{A1b}$$

[1] C. Couteau, S. Barz, T. Durt, T. Gerrits, J. Huwer, R. Prevedel, J. Rarity, A. Shields, and G. Weihs, Nat. Rev. Phys. **5**, 326 (2023).

[2] Y. Liang and H. Zeng, Sci. China: Phys., Mech. Astron. **57**, 1218 (2014).

[3] M. D. Eisaman, J. Fan, A. Migdall, and S. V. Polyakov, Rev. Sci. Instrum. **82**, 071101 (2011).

[4] Y. F. Chen, D. Hover, S. Sendelbach, L. Maurer, S. T. Merkel, E. J. Pritchett, F. K. Wilhelm, and R. McDermott, Phys. Rev. Lett. **107**, 217401 (2011).

[5] S. M. F. Raupach, I. P. Degiovanni, H. Georgieva, A. Meda, H. Hofer, M. Gramegna, M. Genovese, S. Kück, and M. López, Phys. Rev. A **105**, 042615 (2022).

[6] R. H. Hadfield, Nat. Photon. **14**, 201 (2020).

[7] W. Guo, X. Liu, Y. Wang, Q. Wei, L. F. Wei, J. Hubmayr, J. Fowler, J. Ullom, L. Vale, M. R. Vissers, and J. Gao, Appl. Phys. Lett. **110**, 212601 (2017).

[8] J. N. Ullom and D. A. Bennett, Supercond. Sci. Technol. **28**, 084003 (2015).

[9] X. Gu, A. F. Kockum, A. Miranowicz, Y.-X. Liu, and F. Nori, Phys. Rep. **718–719**, 1 (2017).

[10] Z.-L. Xiang, S. Ashhab, J. Q. You, and F. Nori, Rev. Mod. Phys. **85**, 623 (2013).

[11] A. A. Clerk, K. W. Lehnert, P. Bertet, J. R. Petta, and Y. Nakamura, Nat. Phys. **16**, 257 (2020).

[12] G. Kurizki, P. Bertet, Y. Kubo, K. Mølmer, D. Petrosyan, P. Rabl, and J. Schmiedmayer, Proc. Natl. Acad. Sci. USA **112**, 3866 (2015).

[13] B. R. Johnson, M. D. Reed, A. A. Houck, D. I. Schuster, L. S. Bishop, E. Ginossar, J. M. Gambetta, L. DiCarlo, L. Frunzio, S. M. Girvin, and R. J. Schoelkopf, Nat. Phys. **6**, 663 (2010).

[14] G. Romero, J. J. García-Ripoll, and E. Solano, Phys. Rev. Lett. **102**, 173602 (2009).

[15] A. Poudel, R. McDermott, and M. G. Vavilov, Phys. Rev. B **86**, 174506 (2012).

[16] D. S. Golubev, E. V. Il¡¯ichev, and L. S. Kuzmin, Phys. Rev. Appl. **16**, 014025 (2021).

[17] K. Koshino, K. Inomata, Z. Lin, Y. Nakamura, and T. Yamamoto, Phys. Rev. A **91**, 043805 (2015).

[18] K. Inomata, Z. Lin, K. Koshino, W. D. Oliver, J.-S. Tsai, T. Yamamoto, and Y. Nakamura, Nat. Commun. **7**, 12303 (2016).

[19] J.-C. Besse, S. Gasparinetti, M. C. Collodo, T. Walter, P. Kurpiers, M. Pechal, C. Eichler, and A. Wallraff, Phys. Rev. X **8**, 021003 (2018).

[20] C. H. Wong and M. G. Vavilov, Phys. Rev. A **95**, 012325 (2017).

[21] A. Ghirri, S. Cornia, and M. Affronte, Sensors **20**, 4010 (2020).

[22] S. Kono, K. Koshino, Y. Tabuchi, A. Noguchi, and Y. Nakamura, Nat. Phys. **14**, 546 (2018).

[23] A. Cridland, J. H. Lacy, J. Pinder, and J. Verdú, Photonics **3**, 59 (2016).

[24] R. Lescanne, S. Deléglise, E. Albertinale, U. Réglade, T. Capelle, E. Ivanov, T. Jacqmin, Z. Leghtas, and E. Flurin, Phys. Rev. X **10**, 021038 (2020).

[25] I. Iakoupov, Y. Matsuzaki, W. J. Munro, and S. Saito, Phys. Rev. Res. **2**, 033238 (2020).

[26] G. Romero, J. J. García-Ripoll, and E. Solano, Phys. Scr. **2009**, 014004 (2009).

[27] S. R. Sathyamoorthy, L. Tornberg, A. F. Kockum, B. Q. Baragiola, J. Combes, C. M. Wilson, T. M. Stace, and G. Johansson, Phys. Rev. Lett. **112**, 093601 (2014).

[28] B. Royer, A. L. Grimsmo, A. Choquette-Poitevin, and A. Blais, Phys. Rev. Lett. **120**, 203602 (2018).

[29] P. Navez, A. G. Balanov, S. E. Savel'ev, and A. M. Zagoskin, J. Appl. Phys. **133**, 104401 (2023).

[30] C. Caloz, A. Alù, S. Tretyakov, D. Sounas, K. Achouri, and Z.-L. Deck-Léger, Phys. Rev. Appl. **10**, 047001 (2018).

[31] X. Huang, C. Lu, C. Liang, H. Tao, and Y.-C. Liu, Light: Sci. Appl. **10**, 30 (2021).

[32] J. Zhou, X.-L. Yin, and J.-Q. Liao, Phys. Rev. A **107**, 063703 (2023).

[33] N. R. Bernier, L. D. Tóth, A. Koottandavida, M. A. Ioannou, D. Malz, A. Nunnenkamp, A. K. Feofanov, and T. J. Kippenberg, Nat. Commun. **8**, 604 (2017).

[34] X. Li, L. Xie, and L. F. Wei, Phys. Rev. A **92**, 063840 (2015).

[35] D. Roy, C. M. Wilson, and O. Firstenberg, Rev. Mod. Phys. **89**, 021001 (2017).

[36] J.-T. Shen and S. Fan, Phys. Rev. A **79**, 023837 (2009).

[37] S. He, Q. He, and L. F. Wei, Opt. Express **29**, 43148 (2021).

[38] M.-T. Cheng, J. Xu, and G. S. Agarwal, Phys. Rev. A **95**, 053807 (2017).

[39] X. Li and L. F. Wei, Opt. Commun. **366**, 163 (2016).

[40] Y. Xu, Y. Li, R. K. Lee, and A. Yariv, Phys. Rev. E **62**, 7389 (2000).

[41] T. S. Tsoi and C. K. Law, Phys. Rev. A **78**, 063832 (2008).

[42] A. S. Sheremet, M. I. Petrov, I. V. Iorsh, A. V. Poshakinskiy, and A. N. Poddubny, Rev. Mod. Phys. **95**, 015002 (2023).

[43] D. M. Pozar, *Microwave Engineering*, 4th ed (Wiley, Hoboken, NJ, 2012).

[44] J. D. Brehm, A. N. Poddubny, A. Stehli, T. Wolz, H. Rotzinger, and A. V. Ustinov, npj Quantum Mater. **6**, 10 (2021).

[45] R. Barends, J. Kelly, A. Megrant, A. Veitia, D. Sank, E. Jeffrey, T. C. White, J. Mutus, A. G. Fowler, B. Campbell *et al.*, Nature (London) **508**, 500 (2014).

[46] G. Burkard, T. D. Ladd, A. Pan, J. M. Nichol, and J. R. Petta, Rev. Mod. Phys. **95**, 025003 (2023).

[47] P. H. Ouyang, S. R. He, Y. Z. Wang, Y. Q. Chai, J. X. He, H. Chang, and L. F. Wei, Phys. Rev. Res. **6**, 013236 (2024).

[48] J. M. Martinis, M. H. Devoret, and J. Clarke, Nat. Phys. **16**, 234 (2020).